EasyChair Preprint

№ 9291

Possibilities of Field Formation by Permanent Magnets in Magnetic Stereotactic Systems

Hankun Jiao and Oleg Avrunin

November 9, 2022

Possibilities of Field Formation by Permanent Magnets in Magnetic Stereotactic Systems

Jiao Hunkun
Kharkiv National University of Radio Electronics
Kharkiv, Ukraine
1350829683@qq.com, jiao.hankun@nure.ua

Oleg Avrunin
Kharkiv National University of Radio Electronics
Kharkiv, Ukraine
oleh.avrunin@nure.ua

***Abstract*—In this paper, the possibility of forming a magnetic field from permanent magnets in a magnetic stereotaxic system is introduced. The strength and direction of the magnetic field of the electromagnetic coil and the permanent magnets are calculated by the simulation software, and the non-contact movement of the permanent magnets is studied by the microcontroller.**

Keywords—Stereotaxis, Magnetic field, Coil, Microcontroller, Remote control

I. Magnetic Stereotactic System

Very small implantable permanent magnet guided by a large electromagnetic coil is used as a method to deliver heat therapy to the brain tissue or guide the brain tissue through the brain tissue. This process is called "magnetic stereotactic"[1].

Magnetic stereotaxis is a perspective noninvasive methodology for the treatment of brain tumors and others neurological diseases. The main idea of remote manipulations is powerful gradient magnetic field for guide a surgical instrument along arbitrary trajectory to deepbrain structures. Possibilities of remote controlling of surgical equipment are described[2,3].

For high-precision neurosurgical interventions on the deep structures of the brain, direct mechanical control of a surgical instrument (probe, cannula, electrode) moved along a rectilinear trajectory using a stereotaxic apparatus is traditionally used [4]. The limited surgical access, and in some cases the inaccessibility of deep structures of the brain, high traumatism of the surrounding tissues during operations with multiple guidance do not allow to effectively treat a number of diseases of the extrapyramidal nervous system, localized neoplasms of the brain stem, etc [4-8]. Therefore, a promising direction in stereotaxic neurosurgery has become the methods of non-contact impact on the deep structures of the brain (gamma scalpel, magnetic stereotaxis), which have the ability to reach almost any area inside the brain along an arbitrary trajectory with the least traumatism of the surrounding tissues, and magnetic stereotaxis is universal and the least an invasive methodology for performing surgical interventions on the brain.

Magnetic stereotaxic systems are a method that is in the experimental research stage. The method is based on controlling surgical instruments through an external constant magnetic field and moving on pre-calculated trajectories to achieve non-contact control of surgical instruments entering the brain tissue, ensuring minimal trauma to the brain [8-12].

II. Magnetic Field Strength and Ddirection of a Single Electromagnet

The purpose of the experiment is to calculate the magnetic field strength and direction of a single electromagnetic coil and a miniature NdFeB magnet through simulation software.The simulation software is selected as comsol [13].

Experiment design: First, build the electromagnetic coil and the NdFeB magnet model in three-dimensional space (Fig. 1), then set the parameters in the simulation software comsol according to the real material data required for the experiment, build the geometric model in the software according to the parameters. Set The formulas and equations that need to be used, the calculation results and the selection of appropriate sections are required so that the experimental results can be displayed intuitively.

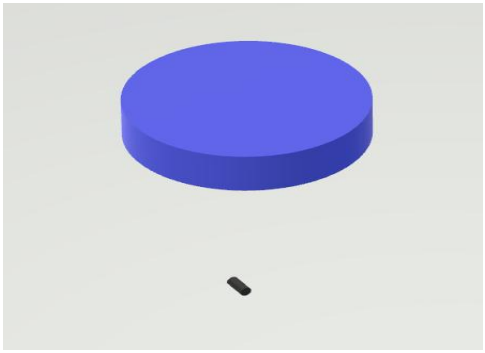

Fig. 1. The blue cylinder is the electromagnetic coil, the black is the NdFeB magnet

A. Parameter settings:

- Electromagnet diameter d_ion=100[mm]=0.1[m]；
- Electromagnet thickness t_ion=30 [mm]=0.03[m];
- Magnetizing strength of electromagnet B_ion=1 [T];
- NdFeB magnet diameter d_NFB =1[mm]=0.001[m];
- NdFeB magnet length l_NFB=2[mm]=0.002[m];
- Distance from electromagnet to NdFeB dis_ion=100[mm]=0.1[m];

Since the experiment is in a general space, the temperature is room temperature 293.15 [K], and the pressure is standard atmospheric pressure 1 [atm];

A 3D model built with a small permanent magnet as the origin. According to the above parameters, a geometric model is established in the software (Fig. 2).

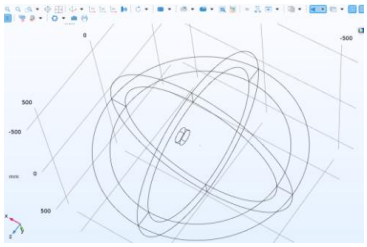

Fig. 2. The larger cylinder is an electromagnet, the smaller one is a NdFeB magnet, the ring around the electromagnet represents infinite space.

B. Material property settings:

1) Electromagnet :

a) Relative permeability μ=4000[1];

b) Conductivity σ=1.12e7[S/m];

c) Relative permittivityεr=1 [1];

d) Residual flux density norm B_ion;

2) NdFeB magnet :

*a) Conductivity σ=1/1.4[uohm*m][S/m];*

b) Relative permittivityεr=1 [1];

c) Recovery permeability μrec=1.05;

d) Residual flux density norm normBr=1.44[T];

The above parameters are all assignments except that they can be changed according to actual experimental needs.

C. The formula involved in the simulation experiment：

The magnetic field produced by a steady current can be calculated from a fixed version of Maxwell-Ampère's law [15].

$$\nabla \times H = J \tag{1}$$

$$\nabla \times B = \mu_0 J \tag{2}$$

where: H - magnetic field intensity,
B - the magnetic flux density,
J - the current density, and
μ_0 - the vacuum permeability,
∇is - hamiltonian.

Gauss's law of magnetic fields predicts the absence of magnetic charges. Another corollary from this law is that the magnetic flux density is spiral, or divergent-free. This means that the magnetic field can be written as the curl of other vector fields as follows:

$$B = \nabla \times A \tag{3}$$

A is vector magnetic potential;

Materials where the current density is proportional to the electric field are described by the constitutional equation known as Ohm's law:

$$J = \sigma E \tag{4}$$

Where J is the current density, σ is is the electric conductivity expressed, E is Electric field intensity;

Constitutive relation B-H:

$$B = \mu_0 \mu_{rec} H + B_r \tag{5}$$

$$B_r = \|B_r\| \frac{e}{\|e\|} \tag{6}$$

Where B is the magnetic flux density, μ_0 is the vacuum permeability, μ_{rec} is recoil permeability, B_r is residual flux density, $\|B_r\|$ is residual flux density norm， e is residual flux direction.

D. Software calculation results

1) Magnetic field strength distribution

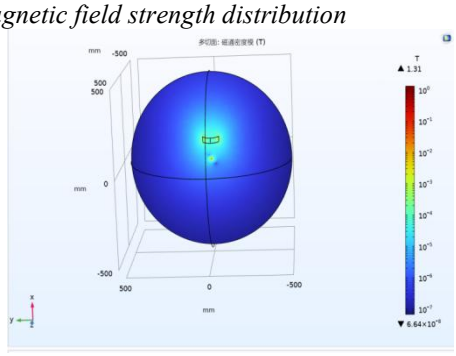

Fig. 3. The distribution of the magnetic field strength in the cross section with the Z-axis;

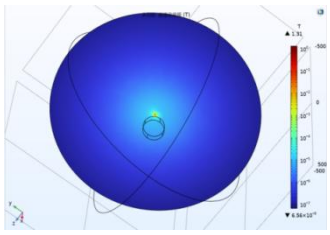

Fig. 4. The distribution of the magnetic field strength in the cross section with the X-axis:

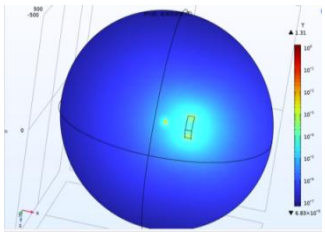

Fig. 5. The distribution of the magnetic field strength in the cross section with the Y-axis:

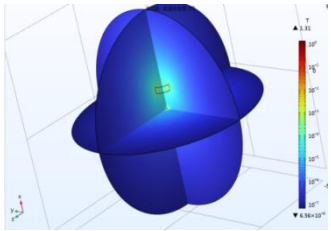

Fig. 6. Magnetic field intensity distribution map (section is X-axis, Y-axis, Z-axis)：

2) The distribution of magnetic field lines:

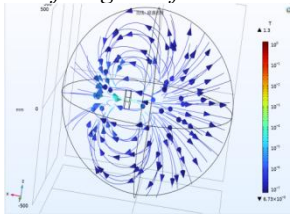

Fig. 7. The arrow is the direction of the magnetic field line, and the streamline is the magnetic flux density.

3) Cross-sectional magnetic field distribution:

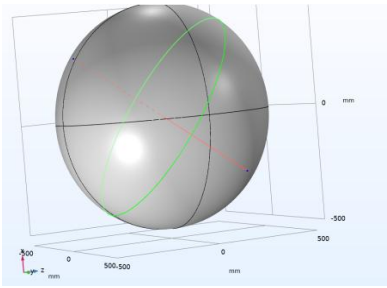

Fig. 8. Selected section:

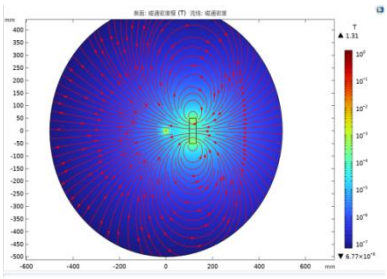

Fig. 9. Magnetic field distribution:

Surface: magnetic flux density mode; streamlines: magnetic flux density; arrows: direction of magnetic field lines.

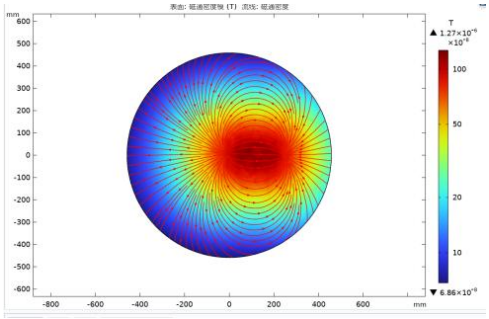

Fig. 10. Top section magnetic field distribution:

Surface: magnetic flux density mode; streamlines: magnetic flux density; arrows: direction of magnetic field lines.

4) Cross-Line Magnetic Field Strength Distribution;

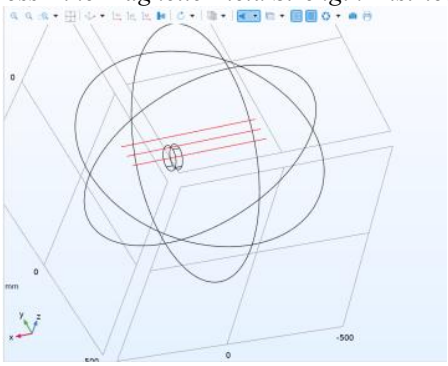

Fig. 11. Select stub:

In the 3D model established with the small permanent magnet as the origin, three stubs are set. These three stubs are parallel to the x-axis in the 3D model, and the distances from the x-axis are 0, 50, and 100 mm respectively. In the line graph, the x-axis is the X-coordinate axis, and the y-axis is the magnetic flux density modulus.

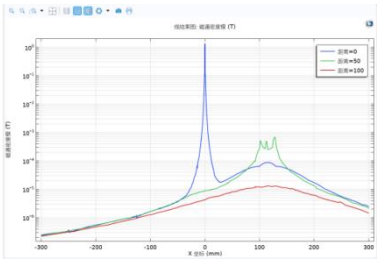

Fig. 12. Cross-sectional line graph of magnetic field intensity distribution:

The line graph shows the magnetic flux density mode on the selected three-dimensional section, the blue line is the distribution of the magnetic flux density mode on the stub at a distance of 0mm from the X-axis, and the green lineis the distribution of the magnetic flux density mode on the stub at a distance of 50mm from the X-axis, and the red lineis the distribution of the magnetic flux density mode on the stub at a distance of 100mm from the X-axis.

Through the simulation experiment using comsol software, we can clearly see the mutual interference of the electromagnet and the magnetic field of the NdFeB magnet, which means that we can make the NdFeB magnet generate spatial displacement by controlling the electrification of the electromagnet, which makes the The idea of multiple electromagnets controlling the trajectory of the NdFeB magnets becomes feasible.

III. Electric Drive - Which Controls the Movement of the Magnet

In order to realize the non-contact movement of the permanent magnet, we choose to build a platform driven by a motor and carry a powerful electromagnet. After the electromagnet is energized, it has a continuous attraction to the permanent magnet, and the arduino [16-18] controls the operation of the motor to control the platform equipped with the electromagnet. move, so as to realize the non-contact movement of the permanent magnet.

The platform is composed of a ball screw slide [19] with a stepping motor, the effective running distance is 300mm, the screw precision is 0.05 mm, and the slide table uses 57x56 stepper motor [20].

The stepper motor has four wires, they need to be connected to the stepper motor controller, the red wire is connected to A+, the green wire is connected to A-, the yellow wire is connected to B+, and the blue wire is connected to B-.The V+ of the external power supply is connected to the V+ of the stepper motor controller, and the V- of the external power supply is connected to the GND of the stepper motor controller. The stepper motor needs to be controlled by arduino [21], so the stepper motor controller must have 3 wires connected to the Arduino control board, the three wires are: PUL, DIR, ENA. Common anode connection method: connect PUL+ DIR+ ENA+ in series, and then connect to the 5V power supply pin of Arduino, PUl- DIR- are connected to the control pins of the Arduino board respectively, and the remaining ENA- can be connected to 5V, Or leave it in the air. Common cathode connection method: Contrary to the above connection method, that is, PUL-, DIR-, ENA- are connected together, and then connected to the GND of Arduino.

This example adopts the common cathode connection method:

- Connect PUL-, DIR-, ENA- together, and then connect to Arduino's GND.
- PUL+ is connected to pin 9 of Arduino and controls the stepper rotation.
- DIR+ is connected to pin 8 of the Arduino and controls the direction of the stepper rotation.
- ENA+ is connected to the GND of Arduino, or can be left unconnected.

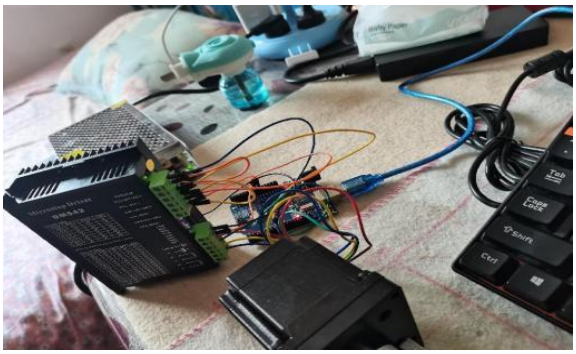

Fig. 13. Stepper motor controller and arduino wiring

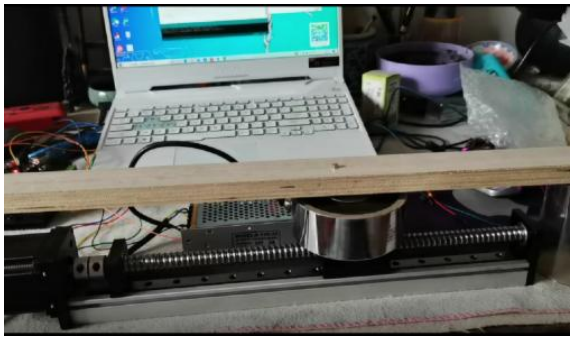

Fig. 14. The slide table is equipped with an electromagnet to control the movement of the permanent magnet

The electromagnet is fixed on the sliding table, and the motor rotates after the power is turned on, which drives the sliding table and the electromagnet to move at a uniform speed. The permanent magnet is affected by the magnetic field of the electromagnet and moves with the slide. It has been proved by many experiments that this method can make the permanent magnet move in a controlled manner without contact. This approach makes it possible to form a strong magnetic field without using expensive and difficult-to-maintain superconducting coils. It can be used not only in stereotactic neurosurgery, but also in the formation of the magnetic-acoustic effect [22-25] for promising technologies of minimally invasive therapy.

REFERENCES

[1] Howard M A, Mayberg M, Grady M S, et al. Magnetic stereotactic system for treatment delivery: U.S. Patent 5,125,888[P]. 1992-6-30.

[2] Howard M A, Mayberg M, Grady M S, et al. Magnetic stereotactic system for treatment delivery: U.S. Patent 5,779,694[P]. 1998-7-14.

[3] Howard M A, Mayburg M, Grady M S, et al. Magnetic stereotactic system for treatment delivery: U.S. Patent 6,216,030[P]. 2001-4-10.

[4] Avrunin, O., Tymkovych, M., Semenets, V., & Piatykop, V. (2019). Computed tomography dataset analysis for stereotaxic neurosurgery navigation. Paper presented at the Proceedings of the International Conference on Advanced Optoelectronics and Lasers, CAOL, , 2019-September 606-609. doi:10.1109/CAOL46282.2019.9019459

[5] Avrunin, O. G., Alkhorayef, M., Saied, H. F. I., & Tymkovych, M. Y. (2015). The surgical navigation system with optical position determination technology and sources of errors. Journal of Medical Imaging and Health Informatics, 5(4), 689-696. doi:10.1166/jmihi.2015.1444

[6] Experimental study of the magnetic stereotaxis system for catheter manipulation within the brain / Grady M.S., Howard M.A., Dacey R.G. , Blume W., Lawson M., Werp P., Ritter R.C. // J. Neurosurg.– 2000.– Vol. 93, № 2.– P. 282–288.

[7] Avrunin, O. G., Tymkovych, M. Y., Moskovko, S. P., Romanyuk, S. O., Kotyra, A., & Smailova, S. (2017). Using a priori data for segmentation anatomical structures of the brain. PrzegladElektrotechniczny, 93(5), 102-105. doi:10.15199/48.2017.05.20

[8] R. G. McNeil, R. C. Ritter, B. Wang, M. A. Lawson, G. T. Gillies, K. G. Wika, et al., "Functional design features and initial performance characteristics of a magnetic-implant guidance system for stereotactic neurosurgery", IEEE Trans. Biomed. Eng., vol. 42, pp. 793-801, Aug. 1995.

[9] M. A. Howard, M. S. Grady, R. C. Ritter, G. T. Gillies, E. G. Quate and J. A. Molloy, "Magnetic movement of a brain thermoceptor", Neurosurg., vol. 24, no. 3, pp. 444-448, 1989.

[10] M. A. Howard Jr., R. C. Ritter and M. S. Grady, Video tumor fighting system, Sept. 1989.

[11] M. S. Grady, M. A. Howard, W. C. Broaddus, H. R. Winn, J. A. Jane, R. C. Ritter, et al., "Initial experimental results with a new stereotactic hyperthermia system", Surg. For., vol. XXXIX, pp. 507-509, 1988.

[12] M. S. Grady, M. A. Howard, J. A. Molloy, R. C. Ritter, E. G. Quate and G. T. Gillies, "Preliminary experimental investigation of in vivo magnetic manipulation: Results and potential applications in hyperthermia", Med. Phys., vol. 16, pp. 263-272, Mar./Apr. 1989.

[13] Pryor R W. Multiphysics modeling using COMSOL®: a first principles approach[M]. Jones & Bartlett Publishers, 2009.

[14] Multiphysics C. Introduction to COMSOL multiphysics®[J]. COMSOL Multiphysics, Burlington, MA, accessed Feb, 1998, 9: 2018.

[15] Maxwell J C. VIII. A dynamical theory of the electromagnetic field[J]. Philosophical transactions of the Royal Society of London, 1865 (155): 459-512.

[16] McRoberts M. Beginning arduino[M]. Apress, 2011.

[17] Badamasi Y A. The working principle of an Arduino[C]//2014 11th international conference on electronics, computer and computation (ICECCO). IEEE, 2014: 1-4.

[18] Banzi M, Shiloh M. Getting started with Arduino[M]. Maker Media, Inc., 2022.

[19] Zaeh M F, Oertli T, Milberg J. Finite element modelling of ball screw feed drive systems[J]. CIRP Annals, 2004, 53(1): 289-292.

[20] Pulford Jr R. Linear stepper motor: U.S. Patent 6,756,705[P]. 2004-6-29.

[21] Louis L. working principle of Arduino and u sing it[J]. International Journal of Control, Automation, Communication and Systems (IJCACS), 2016, 1(2): 21-29.

[22] Bondarenko, S. I., Avrunin, O. G., Bondarenko, I. S., Krevsun, A. V., Koverya, V. P., & Rakhimova, M. V. (2020). On the measurements of magnetic nanoparticle concentration in a biological medium using a superconducting quantum magnetometer. Low Temperature Physics, 46(11), 1094-1097. doi:10.1063/10.0002152

[23] Bondarenko, S. I., Avrunin, O. G., Bondarenko, I. S., Krevsun, A. V., Koverya, V. P., & Rakhimova, M. V. (2020). On the measurements of magnetic nanoparticle concentration in a biological medium using a superconducting quantum magnetometer. Fizika Nizkikh Temperatur, 46(11), 1287-1291

[24] Avrunin, O. G., Bondarenko, I. S., I.bondarenko, S., Kuzmenko, Y. V., Pinaieva, O. Y., Kisała, P.,. Luganskaya, S. (2019). Acoustic excitation of electric field in water solution NaCl. Przeglad Elektrotechniczny, 95(4), 158-161. doi:10.15199/48.2019.04.28

[25] Bondarenko, I. S., Avrunin, O. G., Rakhimova, M. V., Bondarenko, S. I., Krevsun, A. V., & Kulish, S. M. (2019). Acoustomagnetic registration of magnetic nanoparticles in a liquid medium. Telecommunications and Radio Engineering (English Translation of Elektrosvyaz and Radiotekhnika), 78(8), 707-714. doi:10.1615/TelecomRadEng.v78.i8.6